Computer Modeling in Engineering & Sciences CMES, vol.123, no.1, pp.257-282, 2020

Seismic Analysis of the Connections of Buried Segmented Pipes

Wei Liu[1, 2, *], Zhaoyang Song[2] and Yunchang Wang[2]

Abstract: Seismic analysis of buried pipes has been one study focus during the last decades, but the systematic seismic research of pipe connections, especially its relationship with the connected straight pipe, is nearly blank. On the basis, the influence of pipe connections on the joint deformations (JDs) of buried segmented pipes is analyzed in detail by considering different parameters, namely, connection shapes, ground conditions, pipe diameters, branch angles, seismic incident angles, and input ground motions. Moreover, an influence coefficient, which measures the influence of pipe connections on pipe JDs, is calculated. Results show that pipe connections can reduce the JDs of segmented pipes by 40%-50%. Furthermore, the JD is more sensitive to the connection shape, ground condition and pipe diameter than the incident angle and characteristics of seismic waves. An influence coefficient of 0.65 is recommended conservatively for the design of the buried segmented pipes.

Keywords: Segmented pipe, pipe connection, seismic analysis, influence coefficient.

1 Introduction

Buried pipe networks, such as gas and water supply networks, invariably suffer from severe damages during strong earthquakes, which reduce urban functions [Sakai, Pulido, Hasegawa et al. (2017)]. Daily and industrial water supply cannot be ensured due to the failure of water pipes. In addition, the disruption of gas pipes will not only cut down gas supply but will also cause secondary disasters, such as fires and explosions. During the 2008 Wenchuan earthquake (M_L=8.0), over 47,000 km of buried water pipes were damaged, thereby resulting in water supply stoppage in 69.6% of the areas in Sichuan Province [Li, Xiao and Huo (2008)]. After the Lushan earthquake in 2013 (M_L=7.0), the daily gas supply in Lushan City decreased from 500 m^3 to 100 m^3 [Ye, Guo, Liu et al. (2013)]. These seismic investigations emphasize the significance of developing an appropriate seismic analysis method for buried pipes.

Seismic damages of buried pipes result from either permanent ground deformation or seismic wave propagation (SWP) [Shi (2015)]. Investigations after earthquakes indicate that most damages on pipes are caused by SWP; hence, this phenomenon has received more attention

[1] State Key Laboratory of Disaster Reduction in Civil Engineering, Tongji University, Shanghai, 200092, China.

[2] Department of Structural Engineering, Tongji University, Shanghai, 200092, China.

[*] Corresponding Author: Wei Liu. Email: liuw@tongji.edu.cn.

Received: 09 May 2019; Accepted: 12 August 2019.

from researchers than permanent ground deformation. For buried segmented pipes, joint damage is the major cause of failure given that joint stiffness is less than pipe body stiffness. Therefore, the quantization of axial joint deformation (JD) is a priority problem in seismic analysis of buried segmented pipes and hence the major concern in the paper.

The identical deformation method was first proposed by Newmark et al. [Newmark (1967); Newmark and Rosenblueth (1971)] to evaluate the seismic response of buried segmented pipes. In this method, the pipe deformation is assumed to be the same as that of the surrounding soil, and pipe inertia force is neglected. Wang [Wang (1979)] further assumed that pipe body stiffness was considerably greater than joint stiffness and JD was equal to the deformation of soil between the midpoints of two adjacent pipe segments. Shinozuka et al. [Shinozuka and Koike (1979)] introduced a transfer coefficient below 1 to further reflect slippage between pipe and soil. The coefficient depends on pipe strain, wavelength, pipe axial stiffness, and pipe-soil spring stiffness. The transfer coefficient method has been used in the codes of many countries due to its simplicity [Japan Water Works Association (2009); Ministry of Construction of the People's Republic of China (2003)]. However, the aforementioned methods regard input ground motions as simple sinusoidal passage waves and fail to show the nonlinear interaction between soil and pipe. To overcome the drawbacks, quasi-static analytical methods have been proposed and developed by many scholars [Gan and Hou (1988); Wang and Cheng (1979); Wang, Pikul and O'Rourke (1982)]. In accordance with these methods, JDs can be obtained by considering the nonlinear interaction between soil and pipe. Meanwhile, pipe inertia force and soil damping are not considered. At present, dynamic analytical and finite element methods have been extensively used by many scholars to model the complex interaction between pipe and soil [Hindy and Novak (1980); Nelson and Weidlinger (1979); Wang and Lin (1988)]. In addition, integrative modeling theory is an emerging method for analyzing the JDs of buried segmented pipes [Liu, Sun, Miao et al. (2015); Wang and Lau (1989)]. Physical-based stochastic ground motion can be generated as the input by using this model. Furthermore, the entire pipe network with a complex boundary condition and interaction between pipe and soil can be precisely simulated.

In addition to theoretical methods, experiments are widely used to investigate the JDs of buried segmented pipes. For example, indoor tests are frequently designed to examine the basic mechanical behavior of joints, such as the force-displacement relationship of joints and joint strength [Han, Song, Zhang et al. (2010); Singhai (1984)]. Moreover, a full-scale field test is a good method for determining JDs [Miao, Liu, Wang et al. (2016); Wang, Liu and Li (2015)]. Experimental methods are not summarized herein, and additional details can be found in Wang et al. [Wang, Liu and Li (2015)].

For buried segmented pipes, pipe segments are joined by connections with different shapes, such as cruciform, T-shaped, and L-shaped. Although connections can be modeled by several joints, their deformation is not the same as that of straight pipes due to the influence of branch pipes. Therefore, the systematic seismic analysis of pipe connections is necessary. However, O'Rourke et al. [O'Rourke and Liu (1999)] pointed out that studies on this aspect were nearly nonexistent. In limited studies, the ratio of the seismic response of a pipe connection to that of a straight pipe is between 0.1 and 3, which is difficult to be referenced in engineering design [Wang (2015)]. At present, the general solution for this problem is

to refer to relevant works on continuous pipes. For example, Shinozuka et al. [Shinozuka and Koike (1979)] suggested that the additional strain of tees could be calculated by multiplying the strain of straight pipe section by a coefficient larger than one. Liu et al. [Liu and Hou (1990)] summarized the strain adjustment coefficients of different pipe connections based on data investigation. However, whether obtaining the seismic deformation of pipe connections by using the amplification coefficient method is applicable to segmented pipes should be further validated. In this regard, the current study focuses on the seismic analysis of JDs at pipe connections and its relationship with the JDs of straight pipes.

To determine the seismic response of buried segmented pipes, this study first introduces an integrative modeling method proposed by Liu et al. [Liu, Sun, Miao et al. (2015)]. Compared with previous studies, this framework is effective and reliable for the seismic analysis of large buried pipe networks, which has been validated by an artificial earthquake experiment [Liu, Miao, Wang et al. (2017)]. The remaining parts of this paper are organized as follows. Section 3.1 investigates the selection of pipe length in the seismic analysis of a straight ductile cast iron (DCI) pipe. Sections 3.2-3.6 discuss the influences of ground condition, pipe diameter, branch angle, seismic incident angle, and input ground motion on the seismic JDs of DCI pipes with different connection shapes, such as cruciform, T-, K-, L-, and Y-shaped. Moreover, an influence coefficient, which is defined as the ratio of the JD of pipes with connections to that of straight pipes, is calculated. Finally, Section 4 provides the conclusions drawn from this study.

2 Modeling of buried segmented pipes

The dynamic seismic response of buried pipes is insignificant due to the constraint of the surrounding soil [Datta (1999)], which has been validated by field tests [Miao, Liu, Wang et al. (2016)] and theoretical studies [Liu and Li (2008)]. Therefore, inertia and damping forces are typically disregarded for the responses of buried pipes subjected to earthquakes.

The model of beam on elastic foundation (BEF) is widely used in the seismic analysis of buried pipes [Liu, Sun, Miao et al. (2015); Singhal and Zuroff (1990); Wang and Wu (1991); Cao, Zhou, Li et al. (2014); Mandolini and Ruocco (2001)]. In accordance with this model, a buried pipe can be idealized as BEF, as shown in Fig. 1. The axial and lateral motions of the pipe can be described as follows:

$$EA\frac{\partial^2 u(x,t)}{\partial x^2} - k_{\mathrm{A}}u(x,t) = -k_{\mathrm{A}}u_{\mathrm{g}}(x,t) \tag{1}$$

$$EI\frac{\partial^4 v(x,t)}{\partial x^4} + k_{\mathrm{L}}v(x,t) = k_{\mathrm{L}}v_{\mathrm{g}}(x,t) \tag{2}$$

where u (x,t) and v (x,t) are the axial and lateral displacements of the pipe, respectively; u_g (x,t) and v_g (x,t) denote the axial and lateral displacements of ground motion, respectively; EA and EI represent the axial and bending stiffness of the pipe, respectively; E, A, and I refer to the Young's modulus, cross-section area, and inertia module of the pipe, respectively; x stands for the coordinate of the pipe; t is time; and k_{A} and k_{L} are axial and lateral pipe-soil spring stiffness per unit length, respectively, which herein have values

based on the experimental data [Han, Song, Zhang et al. (2010); Sun, Liu and Li (2012, 2012)].

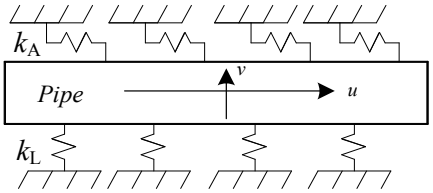

Figure 1: Pipe BEF model

When the pipe is discretized, its element stiffness matrix $[\mathbf{k_P}]$ can be written as follows [Liu, Sun, Miao et al. (2015)]:

$$[\mathbf{k_P}]=\begin{bmatrix} \frac{EA}{L} & 0 & 0 & -\frac{EA}{L} & 0 & 0 \\ 0 & \frac{12EI}{L^3} & \frac{6EI}{L^2} & 0 & -\frac{12EI}{L^3} & \frac{6EI}{L^2} \\ & & \frac{4EI}{L} & 0 & -\frac{6EI}{L^2} & \frac{2EI}{L} \\ & \text{symmetric} & & \frac{EA}{L} & 0 & 0 \\ & & & & \frac{12EI}{L^3} & -\frac{6EI}{L^2} \\ & & & & & \frac{4EI}{L} \end{bmatrix} \tag{3}$$

where L is the length of the element.

The interaction between pipes and the soil that surrounds them can be modeled by axial and lateral springs, and the corresponding stiffness matrix $[\mathbf{k_S}]$ can be written as follows [Wang (1978)]:

$$[\mathbf{k_S}]=\begin{bmatrix} \frac{1}{3}\alpha & 0 & 0 & \frac{1}{6}\alpha & 0 & 0 \\ 0 & \frac{13}{35}\beta & \frac{11}{210}L\beta & 0 & \frac{9}{70}\beta & -\frac{13}{420}L\beta \\ & & \frac{1}{105}L^2\beta & 0 & \frac{13}{420}L\beta & -\frac{1}{140}L^2\beta \\ & \text{symmetric} & & \frac{1}{3}\alpha & 0 & 0 \\ & & & & \frac{13}{35}\beta & -\frac{11}{210}L\beta \\ & & & & & \frac{1}{105}L^2\beta \end{bmatrix} \tag{4}$$

where $\alpha=k_A DL$, $\beta=k_L DL$.

Buried segmented pipes, such as DCI pipes and gray cast iron pipes, are widely used in buried pipe networks. These pipe segments are typically connected by joints, which can be modeled by axial and bending springs [Liu, Sun, Miao et al. (2015)]. The lateral spring exhibits infinite stiffness considering that pipe lateral movement is restrained because one

segment is inserted into another (Fig. 2). Hence, the stiffness matrix of the joint element $[\mathbf{k_J}]$ can be described as follows

$$[\mathbf{k_J}] = \begin{bmatrix} k_{JA} & 0 & 0 & -k_{JA} & 0 & 0 \\ 0 & k_\infty & 0 & 0 & -k_\infty & 0 \\ & & k_{JR} & 0 & 0 & -k_{JR} \\ & \text{symmetric} & & k_{JA} & 0 & 0 \\ & & & & k_\infty & 0 \\ & & & & & k_{JR} \end{bmatrix} \tag{5}$$

where k_{JA} and k_{JR} are the axial and bending spring stiffness of the joint element, respectively; and k_∞ represents the lateral spring with infinite spring stiffness, which has a considerable value.

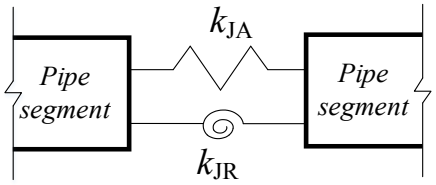

Figure 2: Pipe joint model

Herein, the axial tension and compression behaviors of the joint element are simulated separately due to the different mechanical characteristics in both directions. To simplify, an elastic-plastic model is used for tension behavior and an elastic model is used for compression behavior [Liu, Sun, Miao et al. (2015)]. Fig. 3 illustrates the relationship between the axial force and axial deformation of a joint, where P_u is the ultimate axial-resistant force, Δu_1 represents the ultimate axial deformation at the elastic phase, and Δu_{max} denotes the maximum axial deformation. Herein, the joint compressive stiffness is assumed to equal to the tensile stiffness in the elastic stage for simplification considering both of them originate from the joint material such as rubber gasket, which is isotropy in the compressive and tensile directions.

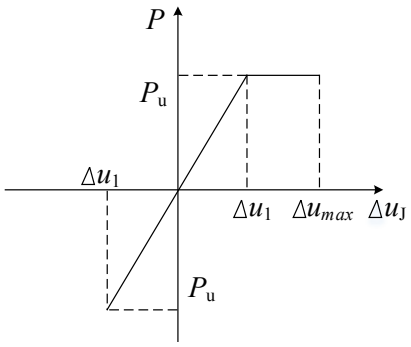

Figure 3: Force-deformation relationship of the axial joint

Notably, the stiffness matrices [$\mathbf{k_P}$], [$\mathbf{k_S}$], and [$\mathbf{k_J}$] are provided in the local coordinate; thus, they should be transformed and assembled in the corresponding system matrices [$\overline{\mathbf{K}}_\mathbf{P}$], [$\overline{\mathbf{K}}_\mathbf{S}$], and [$\overline{\mathbf{K}}_\mathbf{J}$] in the global coordinate. The transformation matrix is as follows:

$$[\mathbf{T}]=\begin{bmatrix} \cos\alpha_T & \sin\alpha_T & 0 & 0 & 0 & 0 \\ -\sin\alpha_T & \cos\alpha_T & 0 & 0 & 0 & 0 \\ 0 & 0 & 1 & 0 & 0 & 0 \\ 0 & 0 & 0 & \cos\alpha_T & \sin\alpha_T & 0 \\ 0 & 0 & 0 & -\sin\alpha_T & \cos\alpha_T & 0 \\ 0 & 0 & 0 & 0 & 0 & 1 \end{bmatrix} \tag{6}$$

where α_T is the angle between the local and global coordinates.

Then, the equation for the pipe network can be expressed as:

$$\left[\overline{\mathbf{K}}_{\mathbf{SYS}}\right]\left\{\overline{\mathbf{u}}\right\}=\left[\overline{\mathbf{K}}_{\mathbf{S}}\right]\left\{\overline{\mathbf{u}}_{\mathbf{g}}\right\} \tag{7}$$

where $\left[\overline{\mathbf{K}}_{\mathbf{SYS}}\right]=\left[\overline{\mathbf{K}}_{\mathbf{P}}\right]+\left[\overline{\mathbf{K}}_{\mathbf{S}}\right]+\left[\overline{\mathbf{K}}_{\mathbf{J}}\right]$ denotes the system general stiffness matrix in the global coordinate; $\left\{\overline{\mathbf{u}}\right\}$ and $\left\{\overline{\mathbf{u}}_{\mathbf{g}}\right\}$ represent the displacement vectors of the pipe element and ground motion in the global coordinate, respectively; the overline symbol "-" of the parameters indicates that they are located in the global coordinate.

Joints are the weakest parts of buried segmented pipes during earthquakes. Thus, among seismic responses, pipe JDs have elicited our interest. Pipe JDs can be readily derived after solving Eq. (7). In fact, if element i is a joint element, then its axial deformation u_J^i and relative rotation angle θ_J^i can be calculated as follows:

$$u_J^i = u_1^{i+1} - u_2^{i-1} \tag{8}$$

$$\theta_J^i = \theta_1^{i+1} - \theta_2^{i-1} \tag{9}$$

where u_1^{i+1} and θ_1^{i+1} are the displacement and rotation angles, respectively, of the left node of element i+1; and u_2^{i-1} and θ_2^{i-1} denote the displacement and rotation angles, respectively, of the right node of element i-1.

3 Seismic analysis of pipe connections of buried segmented pipes

3.1 Finite element model (FEM) of pipe connection

In the FEM of buried segmented pipes with connections, the main components that should be modeled are pipe segments, connections, joints, and pipe-soil interaction. As an example, Fig. 4 shows the detailed information of a cruciform pipe with a length of 27.7 m.

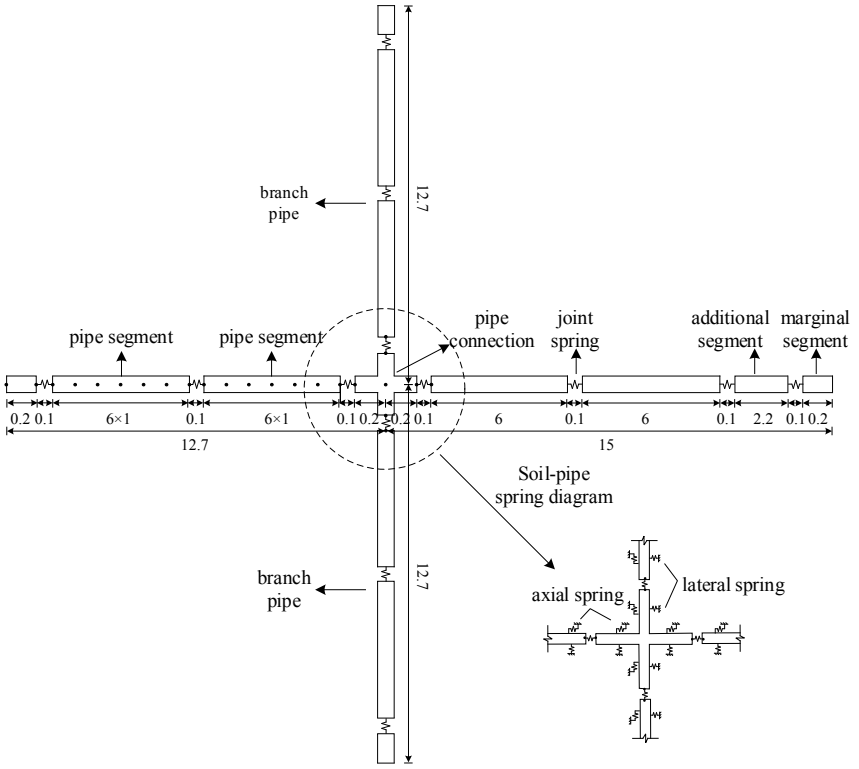

Figure 4: Model of buried segmented pipe with cruciform connection (For showing all components clearly, the figure does not plot strictly according to scale)

In this model, the marginal segments with the length of 0.2 m are located at the ends of pipes. The joint springs have a fixed length of 0.1 m. The pipe segment with a length of 6 m is discretized by six pipe elements with a length of 1 m, which can produce sufficiently accurate results based on our pre-studies. The cruciform connection with a length of 0.4 m is modeled as a whole. The details of pipe-soil springs are also shown in this figure. Notably, if the length of the branch pipe is slightly longer than 12.7 m, e.g., the 15 m right branch pipe in Fig. 4, then 2.3 m remains. In this case, the remaining part is modeled as an additional segment that is less than 6 m, which is located at the end of the pipe and connected with one pipe segment and one marginal segment by joint springs. Moreover, the additional segment is discretized by several pipe elements with a length of 1 m and one element with a length of less than 1 m (2×1 m+0.2 m in this case).

One pipe segment is connected with one axial and one lateral pipe-soil springs to simulate the interaction between pipe and soil. The input ground motion is added to the springs by displacement. In this example, the branch angle, which is defined as the angle between the horizontal and vertical branch pipes, is 90°. This FEM is also applicable to connections with other branch angles or connection shapes, as discussed in each subsection.

3.2 Seismic analysis of straight pipes

The JDs of a straight DCI pipe subjected to earthquake are examined in this subsection. The FEM can be established by using the aforementioned method. As shown in Fig. 5, this model consists of 50 pipe segments (50×6=300 m), 51 joints (51×0.1=5.1 m), 2 marginal segments (2×0.2=0.4 m), and 1 additional segment (0.4 m) connected to the pipe segment by one spring (0.1 m). In addition, the pipe diameter is 0.3 m, and the Young's modulus is 1.5×10^{11} N/m^2. The ground condition is Site II according to the site classifications of the Chinese design code [Ministry of Construction of the People's Republic of China (2003)]. The joint and pipe-soil spring stiffness use values from previous test data [Han, Song, Zhang et al. (2010); Sun, Liu and Li (2012a,b)], i.e., k_A=1.3048×10^8 N/m^2, k_L=6.6940×10^8 N/m^2, k_{JA}=5.685×10^5 N/m^2, and k_{JR}=700 N·m/°.

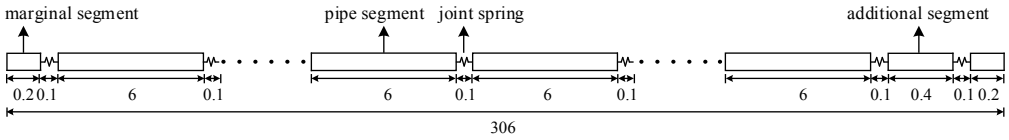

Figure 5: Sketch of straight pipe

The well-known El Centro wave [Pacific Earthquake Engineering Research Center (2017)] is adopted to obtain the seismic responses of buried pipes. The peak acceleration is adjusted to 0.1 g considering the earthquake intensity of VII in the Chinese design code [Ministry of Construction of the People's Republic of China (2003)]. In addition, the seismic incident angle is 45°, and the passage effect of ground motion is considered with propagation velocity of 2000 m/s.

Herein, the maximal JD refers to the maximum JD during the whole earthquake process. In the middle part of the pipe, the maximal JDs are nearly the same, i.e., 0.524 mm (Fig. 6). Herein, the boundary conditions are free. Thus, the maximal JD increases gradually from two ends of the pipe and reaches a stable value at a certain distance (approximately 10 m). The distance varies with different parameters, such as ground condition, pipe diameter, and pipe material. The maximal distances of DCI and steel pipes are approximately 12 m and 65 m, respectively (Fig. 7). Herein, 65 m is selected as the length of the DCI pipe in order to compare the model and analysis results with future works on steel pipes. Therefore, the length of the branch pipe is 153 m, and the influence of boundary conditions can be neglected.

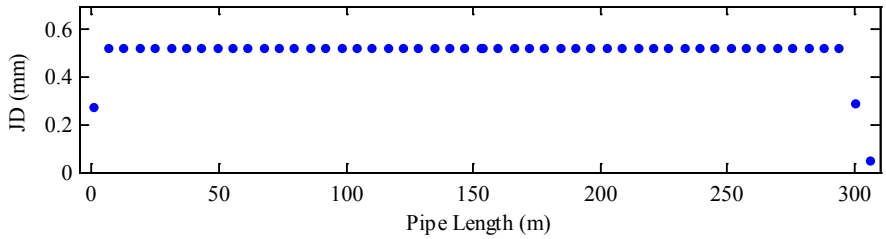

Figure 6: Maximal JD of the straight pipe

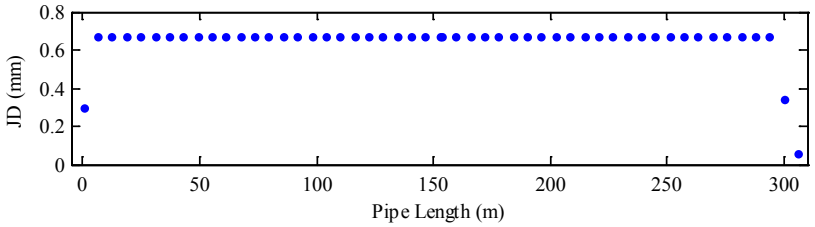

(a) DCI pipe (Site: IV, diameter: 0.3 m, transition distance: 12 m)

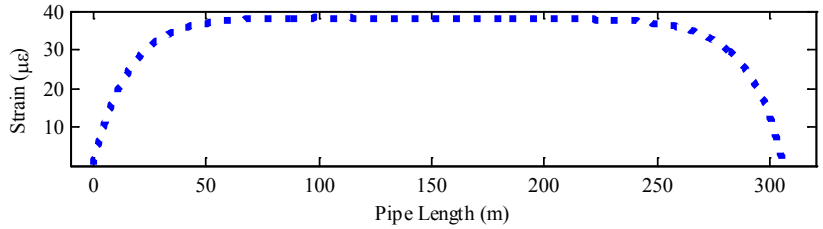

(b) Steel pipe (Site: IV, diameter: 0.4 m, transition distance: 65 m)

Figure 7: Diagram of maximal transition distance for different pipes

3.3 Seismic analysis of the JDs of a cruciform connection

Cruciform connections are widely used in buried pipe networks. They can be regarded as a simple pipe network that is composed of four pipes with a length of 153 m. Fig. 8 shows cruciform connections with different branch angles, namely, 30°, 60°, and 90°. Herein, the connection parts are modeled using the aforementioned method and connected to pipe segments by joint springs.

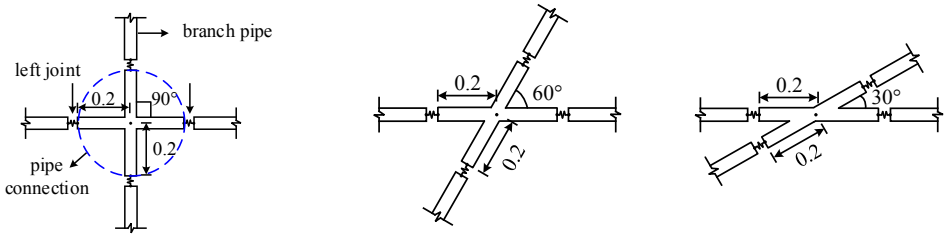

(a) 90° (b) 60° (c) 30°

Figure 8: Cruciform connections with different branch angles

A cruciform connection is connected to pipe segments by left and right joint springs; thus, its deformations are our concern. To avoid the influence of boundary conditions, the influence of pipe length on the two JDs is discussed. Herein, the cruciform connection with a branch angle of 90° is analyzed, and the parameters are the same as those in Section 3.1. As shown in Fig. 9, when the pipe lengths are 184, 306, and 403.6 m, the maximal deformations of the left and right joints are identical (Fig. 8, 0.291 mm), which indicates that 184 m is sufficient to avoid the influence of boundary conditions on the JDs of the cruciform connection. Herein, 306 m is adopted as the pipe length of the cruciform

connection for convenient modeling and comparison with a straight pipe. The JDs along the pipe have the same profiles as those shown in Fig. 9(a); hence, a partially enlarged detail is plotted in the subsequent figures.

The maximal JDs of cruciform connections with different ground motions, branch angles, pipe diameters, seismic incident angles, and input ground motions are examined in detail in the following subsections. The cruciform connection is connected to the pipe segment by left and right joint springs (Fig. 10); therefore, both their maximal JDs are analyzed. Herein, the maximum of the two maximal JDs is selected to study the influence of the connection. In addition, the maximal JDs of a straight pipe in the corresponding position with the same parameters are used as the benchmarks to illustrate the influences of the aforementioned parameters (Fig. 10).

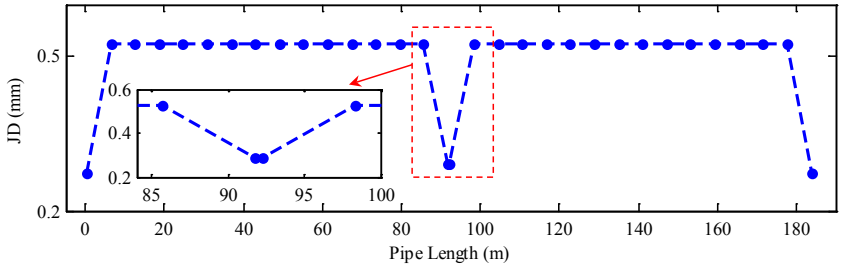

(a) Pipe length=184 m (92 m×2)

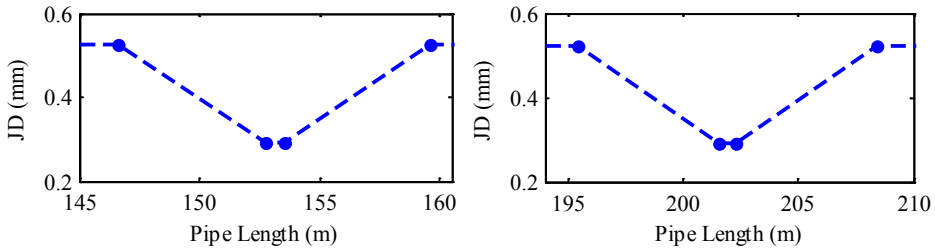

(b) Pipe length=306 m (153 m×2) (c) Pipe length=403.6 m (201.8 m×2)

Figure 9: Maximal JDs of cruciform connection in different length

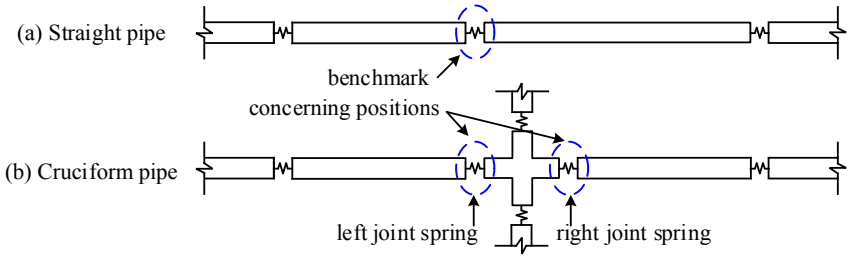

Figure 10: Comparison between straight and cruciform pipes

3.3.1 Different ground conditions

The influence of ground condition on the JDs of the cruciform connection subjected to earthquake (Case C-1) is discussed in this subsection. In Chinese seismic design code, the engineering ground conditions are divided into four types (Site I-IV) based on equivalent shear wave velocity and thickness of overlaying layer [Ministry of Construction of the People's Republic of China (2003)]. Briefly, the ground becomes "solider" when the shear wave velocity becomes greater under the same thickness of overlaying layer. In each ground condition, both axial and lateral pipe-soil spring stiffness values can be calculated by one-dimensional wave motion theory in cylindrical coordinates [Sun, Liu and Li (2012a, b)], which are listed in Tab. 1. Other parameters are provided in the first line of Tab. 2.

Table 1: Axial and lateral pipe-soil spring stiffness in four ground conditions

Site No.	Axial pipe-soil spring stiffness k_A (N/m^2)	Lateral pipe-soil spring stiffness k_L (N/m^2)
I	3.4748×10^8	1.8596×10^9
II	1.3048×10^8	6.6940×10^8
III	5.8969×10^7	2.9753×10^8
IV	1.5890×10^7	7.4362×10^7

Table 2: Parameters of cruciform connection in different cases

Cases	Calculation parameters				
	Site No.	Diameter (m)	Branch angle	Incident angle	Input ground motion
Case C-1	I, II, III, IV	0.3	90°	45°	El-Centro
Case C-2	II	0.15, 0.2, 0.3	90°	45°	El-Centro
Case C-3	II	0.3	30°, 60°, 90°	45°	El-Centro
Case C-4	II	0.3	90°	30°, 45°, 60°	El-Centro
Case C-5	II	0.3	90°	45°	El-Centro, Morgan Hill, Westmorland

As illustrated in Fig. 11(a), the maximal JDs in Site I are the same as those of the straight pipe except for the sharp decline at the left and right joints of the connection. Herein, the maximal JD of the left joint (JD_{left}) is the same as that of the right joint (JD_{right}, 0.221 mm). In Sites II-IV, the JDs of the straight pipe and cruciform connection are similar to those in Fig. 11(a). Therefore, only the partially magnified details, including the three left and three right joints of the cruciform connection, are plotted in the following figures. Herein, an influence coefficient ζ is defined as the ratio of the maximum of JD_{left} and JD_{right} (Fig. 10(b), JD_c) to that of the straight pipe (Fig. 10(a), JD_0) in the corresponding location.

$$\zeta = \frac{JD_c}{JD_0} \tag{10}$$

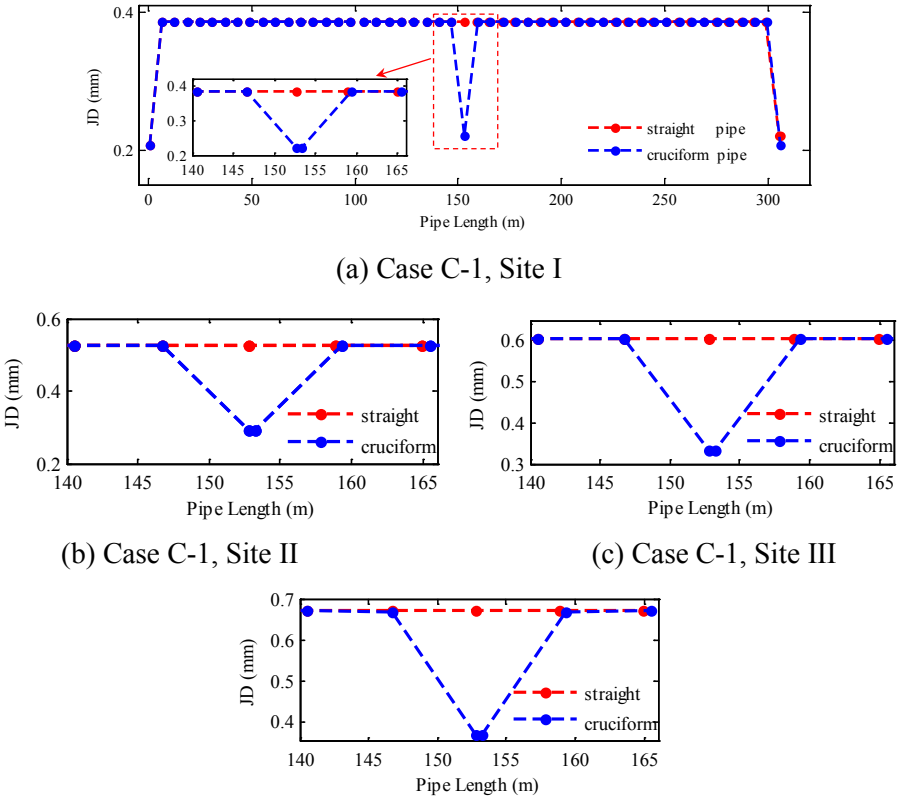

(a) Case C-1, Site I

(b) Case C-1, Site II

(c) Case C-1, Site III

(d) Case C-1, Site IV

Figure 11: Maximal JDs of cruciform pipes in different ground conditions

The influence coefficients in the four ground conditions are listed in Tab. 3. The influence coefficients in this table are all 0.5-0.6, which can be explained qualitatively by using the identical deformation method [Newmark (1967); Newmark and Rosenblueth (1971)]. In accordance with this method, the buried pipes and surrounding soil move together under earthquakes, i.e., they have identical deformation. Despite its simplicity, this method identifies the key factors for the seismic response of buried pipes. The deformation of the surrounding soil Δ_S can be written as follows:

$$\Delta_S = \Delta_P + \Delta_J \tag{11}$$

where Δ_P represents pipe body deformation, and Δ_J denotes JD.

Table 3: Influence coefficients of cruciform connection in four ground conditions

Site No.	JD_0 (mm)	JD_{left} (mm)	JD_{right} (mm)	JD_c (mm)	ζ
I	0.385	0.221	0.221	0.221	0.574
II	0.524	0.291	0.291	0.291	0.555
III	0.606	0.333	0.333	0.333	0.550
IV	0.673	0.368	0.368	0.368	0.547

Joint stiffness is considerably less than pipe body stiffness. Therefore, soil deformation is typically believed to be absorbed by the joint, and thus, is approximately equal to JD ($\Delta_S \approx \Delta_J$). Then, the Δ_S between the midpoints of two adjacent pipe segments for the straight pipe (approximately 6 m, neglecting the length of the joint) is absorbed by one joint (Fig. 12(a)), whereas it is absorbed by two joints (Fig. 12(b)) for the cruciform connection (neglecting the length of the connection and joint). Therefore, the Δ_J of the cruciform connection is theoretically half of that of the straight pipe.

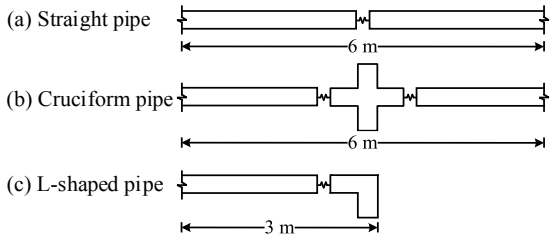

Figure 12: Sketches of identical deformation method

However, the influence coefficients shown in Tab. 3 are all higher than 0.5. The reasons are as follows: (a) the preceding method neglects relative slippage between the pipe and its surrounding soil, whereas the FEM considers this slippage; and (b) branch pipes connected by the same connection may influence one another.

In Tab. 3, JD_0 and JD_c increase significantly from Site I to IV, and the JD ratios in Sites IV and I are 74.8% and 66.5%, respectively. In addition, the influence coefficients tend to decrease as soil becomes soft (from Site I to IV), and the maximal relative error is 4.94%. Soil strain along adjacent pipes is absorbed by the pipe body and joint based on the identical deformation method. The constraint of soil on pipe body weakens with a decrease in pipe-soil spring stiffness from Site I to IV (Tab. 1). Then, the seismic response of the pipe body reduces, and JD increases correspondingly.

3.3.2 Different pipe diameters

The influence of pipe diameter on pipe JD (Case C-2) is investigated in this subsection. Three DCI pipes with diameters of 0.15, 0.2, and 0.3 m are studied because their joint spring stiffness values are available from previous tests [Han, Song, Zhang et al. (2010)]. Tab. 4 lists the parameters of pipe properties, joint and pipe-soil springs. Other parameters are listed in the second line of Tab. 2.

Table 4: Parameters of three pipes

Diameter (m)	k_{JA} (N/m)	k_{JR} (N·m/°)	k_A (N/m^2)	k_L (N/m^2)	Area (m^2)	Moment of inertia (m^4)
0.15	4.064×10^5	90	1.2232×10^8	6.9381×10^8	0.0028	8.9583×10^{-6}
0.20	4.651×10^5	250	1.2561×10^8	6.8548×10^8	0.0040	2.1742×10^{-5}
0.30	5.685×10^5	700	1.3048×10^8	6.6940×10^8	0.0068	8.2015×10^{-5}

As shown in Fig. 13 and Tab. 5, the influence coefficients of the pipes with different diameters are all approximately 0.5-0.6, and they decrease with an increase in pipe diameter. The maximal relative error is 2.88%. The influence coefficient is slightly higher than 0.5 considering that the deformation of the horizontal pipe increases due to the

influence of the branch pipe. In addition, JD_0 and JD_c increase with an increase in pipe diameter. When the diameter is 0.3 m, their values are 0.524 mm and 0.291 mm, respectively, which are 28.4% and 24.9% higher than the values when the diameter is 0.15 m. On the basis of identical deformation theory, when pipe diameter increases, the stiffness of the pipe body increases while the soil remains constant. Therefore, the constraint of soil to the pipe body weakens. Consequently, the deformation of the pipe body decreases, whereas JD increases. Moreover, JD_{left} is the same as JD_{right}, thereby indicating no difference in the influence of the branch pipe on left and right joints of the horizontal pipe.

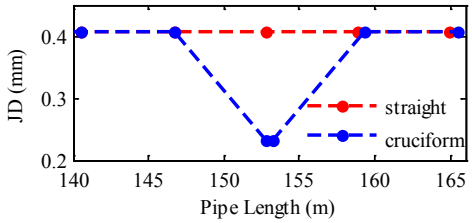

Figure 13: Maximal JDs of cruciform connection (Case C-2, 0.15 m)

Table 5: Influence coefficients of cruciform connection with different diameters

Diameter (m)	JD_0 (mm)	JD_{left} (mm)	JD_{right} (mm)	JD_c (mm)	ζ
0.15	0.408	0.233	0.233	0.233	0.571
0.20	0.457	0.258	0.258	0.258	0.565
0.30	0.524	0.291	0.291	0.291	0.555

3.3.3 Different branch angles

The JDs of the cruciform connection with different branch angles (Case C-3, Fig. 8) are examined in this subsection. The parameters are listed in the third line of Tab. 2. As shown in Fig. 14 and Tab. 6, the influence coefficients of the cruciform connection with different branch angles are all approximately 0.5, which exhibits the favorable influence of a cruciform connection with different branch angles on reducing the seismic response of a pipe. JD_{left} decreases as the branch angle changes from 90° to 30°, whereas JD_{right} increases, due to the influence of the branch pipe. Therefore, the influence coefficients are not exactly 0.5 and tend to increase as the branch angle decreases with a maximal relative error of 8.65%.

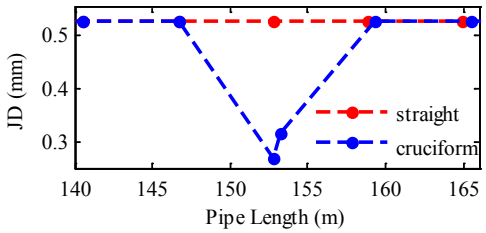

Figure 14: Maximal JDs of cruciform connection (Case C-3, 30°)

Table 6: Influence coefficients of cruciform connection with different branch angles

Branch angle	JD_0 (mm)	JD_{left} (mm)	JD_{right} (mm)	JD_c (mm)	ζ
30°	0.524	0.267	0.316	0.316	0.603
60°	0.524	0.281	0.301	0.301	0.574
90°	0.524	0.291	0.291	0.291	0.555

3.3.4 Different seismic incident angles

Theoretically, the displacement components of input ground motion in the axial and lateral directions of a pipe vary with a change in incident angles, thereby leading to different pipe JDs. Herein, three incident angles, i.e., 30°, 45°, and 60°, are used to examine the influence of incident angle on pipe JDs (Case C-4). The calculation parameters are listed in the fourth line of Tab. 2. As shown in Fig. 15 and Tab. 7, although JD_0 and JD_c vary with a change in incident angle, all the influence coefficients of the cruciform pipe are 0.555. Therefore, the influence of seismic incident angle on the influence coefficients of a cruciform pipe can be neglected.

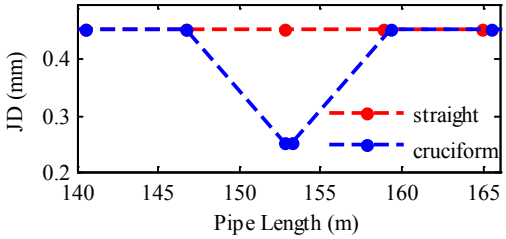

Figure 15: Maximal JDs of cruciform connection (Case C-4, 30°)

Table 7: Influence coefficients of cruciform connection under different incident angles

Incident angle	JD_0 (mm)	JD_{left} (mm)	JD_{right} (mm)	JD_c (mm)	ζ
30°	0.454	0.252	0.252	0.252	0.555
45°	0.524	0.291	0.291	0.291	0.555
60°	0.454	0.252	0.252	0.252	0.555

3.3.5 Different input ground motions

To examine the influence of other input ground motions, the JDs of the straight pipe and cruciform connection subjected to three input ground motions (Case C-5), namely, El Centro, Morgan Hill, and Westmorland waves [Pacific Earthquake Engineering Research Center (2017)], are analyzed. Other parameters are listed in the fifth line of Tab. 2. As shown in Fig. 16 and Tab. 8, all the influence coefficients that are subjected to the three waves are approximately 0.5, which indicates that the cruciform connection will reduce pipe JDs regardless of the input ground motion. In addition, although JD_0 and JD_c vary evidently due to the different displacement peaks and wave shapes of the three ground motions, the corresponding influence coefficients are nearly the same. Therefore, the waves significantly influence pipe JDs, but only slightly affect the influence coefficients.

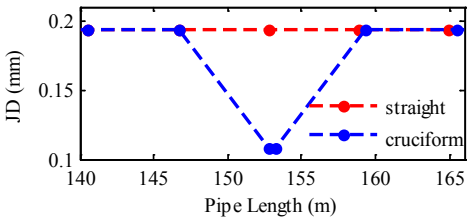

Figure 16: Maximal JDs of cruciform connection (Case C-5, Westmorland wave)

Table 8: Influence coefficients of cruciform connection under different input ground motions

Input ground motion	JD_0 (mm)	JD_{left} (mm)	JD_{right} (mm)	JD_c (mm)	ζ
El-Centro	0.524	0.291	0.291	0.291	0.555
Morgan Hill	0.119	0.066	0.066	0.066	0.553
Westmorland	0.194	0.108	0.108	0.108	0.557

The influence coefficients of different cases are summarized in Tab. 9. Obviously, all influence coefficients are approximately 0.5, which indicates that the cruciform connection will reduce pipe JD. Furthermore, ground condition, pipe diameter, and branch angle exert larger influence coefficients than seismic incident angle and input ground motion. Therefore, the influence coefficient of the connection is suggested to have a value of 0.65 for safety and simplification, thereby neglecting the effects of the parameters in Tab. 9. For the cruciform connection with different parameters, the sum of the left and right JDs is larger than that of the straight pipe (Sections 3.2.1-3.2.5), which may be attributed to the influence of the branch pipe.

Table 9: Influence coefficients of cruciform connection in different cases

Cases	Influence coefficients range	Maximum relative error
Case C-1	0.547-0.574	4.94%
Case C-2	0.555-0.571	2.88%
Case C-3	0.555-0.603	8.65%
Case C-4	0.555	0
Case C-5	0.553-0.557	0.72%

3.4 Seismic analysis of the JDs of a T-shaped connection

Pipes with T-shaped connections are common at the end of one network. Similar to a cruciform connection, a T-shaped connection can be modeled by three branch pipes that are connected by a tee. As suggested in Section 3.2, the influence of boundary conditions can be avoided when the lengths of the three pipes are all 153 m. Herein, three branch angles, i.e., 30°, 60°, and 90°, are considered as shown in Fig. 17. Similar to the cruciform connection, the influences of ground conditions, pipe diameters, branch angles, seismic incident angles, and input ground motions are investigated. Furthermore, JD_{left} and JD_{right} are considered (Fig. 17 (a)), and the influence coefficient is calculated using Eq. (10).

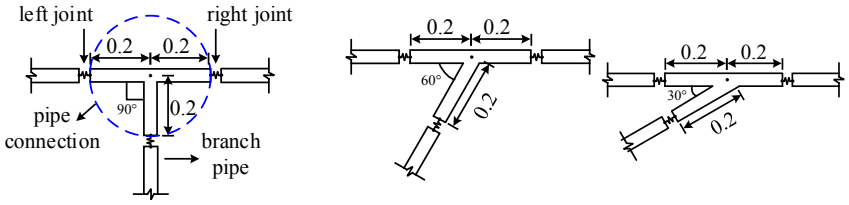

(a) 90° (b) 60° (c) 30°

Figure 17: T-shaped connections with different branch angles

(1) Different ground conditions

Four ground conditions (i.e., Site I-IV) are considered to analyze the influence of ground condition on the JD of a T-shaped pipe (Case T-1). The axial and lateral pipe–soil spring coefficients in the four ground conditions are provided in Tab. 1, and other parameters are listed in the first line of Tab. 10. The maximal JDs in Site II are used as an example and shown in Fig. 18(a). All the influence coefficients are presented in the first line of Tab. 11.

Table 10: Calculation parameters of T-shaped connection in different cases

Cases	Calculation parameters				
	Site No.	Diameter (m)	Branch angle	Incident angle	Input ground motion
Case T-1	I, II, III, IV	0.3	90°	45°	El-Centro
Case T-2	II	0.15,0.2,0.3	90°	45°	El-Centro
Case T-3	II	0.3	30°, 60°, 90°	45°	El-Centro
Case T-4	II	0.3	90°	30°, 45°, 60°	El-Centro
Case T-5	II	0.3	90°	45°	El-Centro, Morgan Hill, Westmorland

(2) Different diameters

To illustrate the influence of pipe diameter on the JD of the T-shaped connection (Case T-2), three pipe diameters (0.15, 0.2, and 0.3 m) are examined. Pipe properties and joint and pipe-soil springs are provided in Tab. 4. Other parameters are listed in the second line of Tab. 10. In addition, the maximal JDs when the pipe diameter is 0.2 m are used as an example and shown in Fig. 18(b). All the influence coefficients are listed in the second line of Tab. 11.

(3) Different branch angles

As shown in Fig. 17, three branch angles (i.e., 30°, 60°, and 90°) are selected to study the influence of branch angle on the JD of the T-shaped connection (Case T-3). Other parameters are listed in the third line of Tab. 10. The maximal JDs are shown in Fig. 18(c) using the branch angle of 60° as an example. All the influence coefficients are listed in the third line of Tab. 11.

(4) Different seismic incident angles

Three seismic incident angles, i.e., 30°, 45°, and 60°, are considered to illustrate the influence of incident angle on the JD of the T-shaped connection (Case T-4). Other parameters are

listed in the fourth line of Tab. 10. Fig. 18(d) shows the maximal JDs when the incident angle is 30°. All the influence coefficients are listed in the fourth line of Tab. 11.

(5) Different input ground motions

Three input ground motions are considered (Case T-5), including El Centro, Morgan Hill, and Westmorland waves (PEER, 2017). Other parameters are listed in the fifth line of Tab. 10. Fig. 18(e) presents the maximal JDs subjected to the Westmorland wave. All the influence coefficients are listed in the fifth line of Tab. 11.

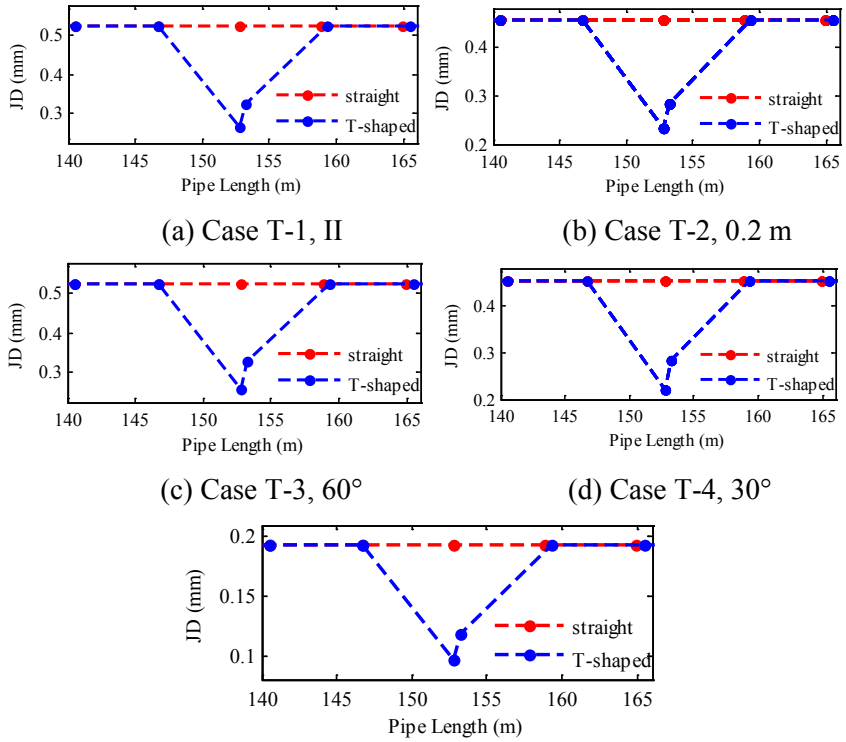

(a) Case T-1, II (b) Case T-2, 0.2 m

(c) Case T-3, 60° (d) Case T-4, 30°

(e) Case T-5, Westmorland wave

Figure 18: Maximal JDs of T-shaped connection under different parameter

Table 11: Influence coefficients of T-shaped connection in different cases

Cases	Influence coefficients range	Maximum variability
Case T-1	0.603-0.644	6.78%
Case T-2	0.615-0.625	1.63%
Case T-3	0.615-0.624	1.46%
Case T-4	0.615-0.623	1.30%
Case T-5	0.612-0.615	0.49%

As shown in Tab. 11, although the influence coefficients vary within a certain range, they are all less than one, which indicates that the T-shaped connection will reduce pipe JD.

Similar to that of the cruciform connection, this beneficial effect of the T-shaped connection can be explained by using the identical deformation method. All the influence coefficients are higher than 0.5; thus, the branch pipe of the T-shaped pipe actually increases connection JD more evidently than the cruciform connection (Tab. 9). In addition, from the perspective of influence coefficient variability, the influence of ground condition (6.78%) is more noticeable than those of pipe diameter (1.63%), branch angle (1.46%), and seismic incident angle (1.30%), whereas the influence of different input ground motions (0.49%) can be neglected. Moreover, JD_{left} is less than JD_{right} due to the asymmetrical arrangement of the T-shaped connection. As suggested in Section 3.2, the connection safety of T-shaped pipes can be guaranteed when the influence coefficient has a value of 0.65.

3.5 Seismic analysis of the JDs of a K-shaped connection

Fig. 19 shows widely used K-shaped connections with three branch angles, i.e., 30°, 45°, and 60°. Their FEMs are the same as those of the cruciform and T-shaped connections. The influences of ground conditions, pipe diameters, branch angles, seismic incident angles, and input ground motions on the maximal JDs and the influence coefficients of the K-shaped pipes (Cases K-1-5) are discussed in this section. Similar to the T-shaped connection, the joint and pipe-soil springs are shown in Tabs. 1 and 4. Other parameters that correspond to the five cases are listed in Tab. 12. Examples of the maximal JDs of the K-shaped connection and straight pipe under different parameters are shown in Fig. 20. The influence coefficients are provided in Tab. 13.

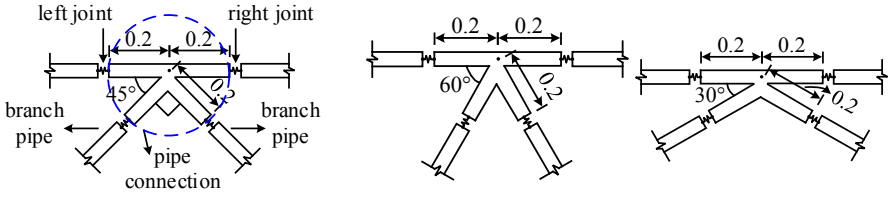

(a) 45° (b) 60° (c) 30°

Figure 19: K-shaped connections with different branch angles

Table 12: Calculation parameters of K-shaped connection in different cases

Cases	Calculation parameters				
	Site No.	Diameter (m)	Branch angle	Incident angle	Input ground motion
Case K-1	I, II, III, IV	0.3	90°	45°	El-Centro
Case K-2	II	0.15, 0.2, 0.3	90°	45°	El-Centro
Case K-3	II	0.3	30°, 45°, 60°	45°	El-Centro
Case K-4	II	0.3	90°	30°, 45°, 60°	El-Centro
Case K-5	II	0.3	90°	45°	El-Centro,Morgan Hill, Westmorland

Table 13: Influence coefficients of K-shaped connection in different cases

Cases	Influence coefficients range	Maximum variability
Case K-1	0.605-0.644	6.45%
Case K-2	0.615-0.625	1.63%
Case K-3	0.615-0.616	0.16%
Case K-4	0.615-0.626	1.79%
Case K-5	0.613-0.615	0.33%

Similar to the T-shaped connection, the K-shaped connection helps reduce pipe JD, but the influence coefficients are all slightly higher than 0.6 (Tab. 13). Among the five cases, the influence of ground condition is more evident than those of pipe diameter and seismic incident angle, whereas the influences of branch angle and input ground motion can be neglected. Moreover, JD_{left} is less than JD_{right} as shown in Fig. 20. In addition, an influence coefficient of 0.65 is reasonable for designers.

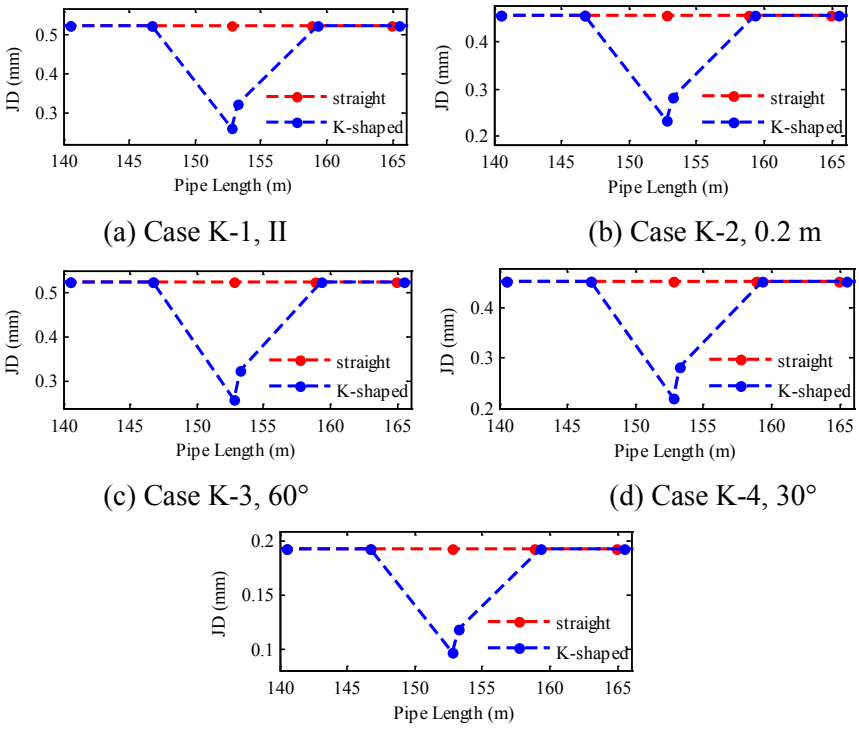

Figure 20: Maximal JDs of K-shaped connection under different parameters

3.6 Seismic analysis of the JDs with an L-shaped connection

Pipes with L-shaped connections are frequently located at the corners of a network. Similar to the cruciform, T-shaped, and K-shaped connections, the L-shaped connection is connected to pipe segments by joint springs. However, the pipe segment and connection in the horizontal direction are connected by only one joint (Fig. 21). The influences of the parameters on the JD of the L-shaped connection (Cases L-1-5) are discussed in this section. The parameters of the five cases are listed in Tab. 14. Herein, three branch angles of the L-shaped connection, i.e, 30°, 60°, and 90°, are considered (Fig. 21). Fig. 22 presents samples of the results and Tab. 15 summarizes the influence coefficients.

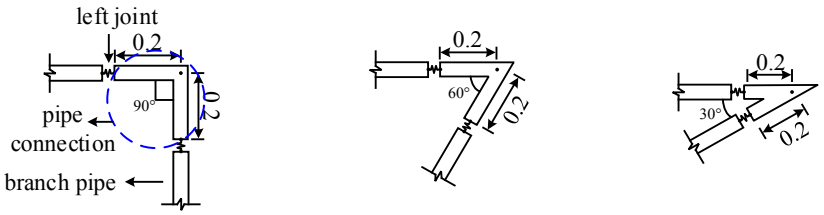

(a) 90° (b) 60° (c) 30°

Figure 21: L-shaped connections with different branch angles

Table 14: Calculation parameters of L-shaped connection in different cases

Cases	Calculation parameters				
	Ground condition	Diameter (m)	Branch angle	Incident angle	Input ground motion
Case L-1	I, II, III, IV	0.3	90°	45°	El-Centro
Case L-2	II	0.15, 0.2, 0.3	90°	45°	El-Centro
Case L-3	II	0.3	30°, 60°, 90°,	45°	El-Centro
Case L-4	II	0.3	90°	30°, 45°, 60°	El-Centro
Case L-5	II	0.3	90°	45°	El-Centro, Morgan Hill, Westmorland

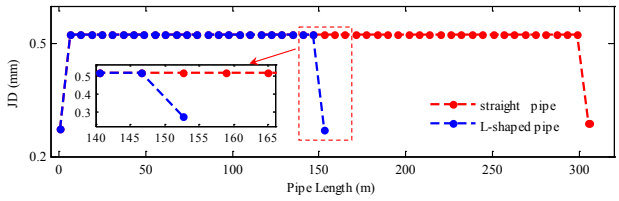

(a) Case L-1, II

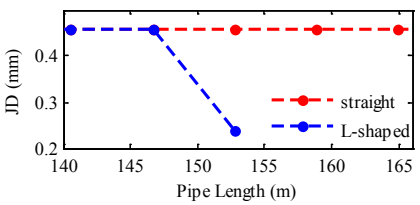

(b) Case L-2, 0.2 m

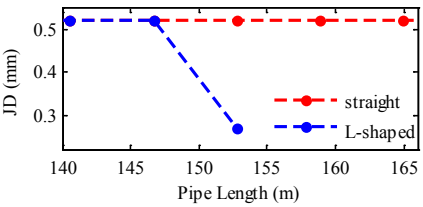

(c) Case L-3, 60°

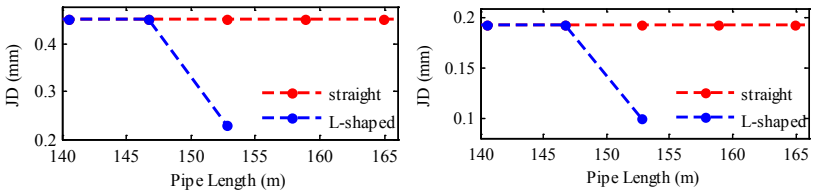

(d) Case L-4, 30° (e) Case L-5, Westmorland

Figure 22: Maximal JDs of L-shaped connection in different parameters

Table 15: Influence coefficients of L-shaped connection in different cases

Cases	Influence coefficient	Maximum variability
Case L-1	0.506-0.530	4.74%
Case L-2	0.517-0.532	2.90%
Case L-3	0.513-0.517	0.78%
Case L-4	0.509-0.517	1.57%
Case L-5	0.515-0.517	0.39%

Results show that the L-shaped connection decreases pipe JD. The influence coefficients under different parameters are approximately 0.5, which can also be explained by identical deformation theory as described in Section 3.2. For the L-shaped connection, the JD within the half pipe segment is borne by one joint as shown in Figs. 12(a) and 12(c). Hence, the influence coefficient in Eq. (10) is approximately 0.5. Furthermore, the influences of ground condition and pipe diameter on the influence coefficients are more significant than those of the other parameters. Moreover, when the influence coefficient is 0.65 as suggested in Section 3.2, pipe connection is safe in engineering applications.

3.7 Seismic analysis of the JDs of a Y-shaped connection

Pipes with Y-shaped connections commonly exist in the middle part of a network. Their FEMs are shown in Fig. 23. Similarly, the influences of the parameters on the JDs of the Y-shaped connections (Cases Y-1-5) are analyzed in this section. The corresponding parameters are listed in Tab. 16. The Y-shaped connections with three different branch angles are shown in Fig. 23. The partial analysis results are provided in Fig. 24, and all the influence coefficients are summarized in Tab. 17.

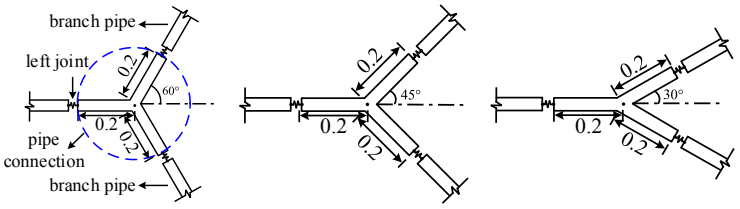

(a) 60° (b) 45° (c) 30°

Figure 23: Y-shaped connections with different branch angles

Table 16: Calculation parameters of Y-shaped connection in different cases

Cases	Calculation parameters				
	Site No.	Diameter (m)	Branch angle	Incident angle	Input ground motion
Case Y-1	I, II, III, IV	0.3	90°	45°	El-Centro
Case Y-2	II	0.15, 0.2, 0.3	90°	45°	El-Centro
Case Y-3	II	0.3	30°, 45°, 60°	45°	El-Centro
Case Y-4	II	0.3	90°	30°, 45°, 60°	El-Centro
Case Y-5	II	0.3	90°	45°	El-Centro, Morgan Hill, Westmorland

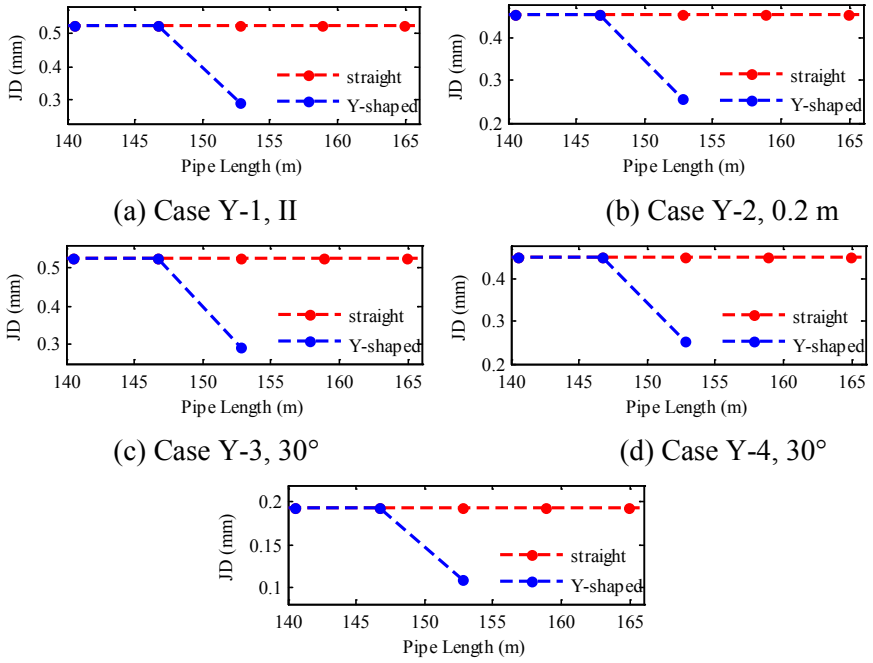

(a) Case Y-1, II

(b) Case Y-2, 0.2 m

(c) Case Y-3, 30°

(d) Case Y-4, 30°

(e) Case Y-5, Westmorland

Figure 24: Maximal JDs of Y-shaped connection under different parameters

Table 17: Influence coefficients of Y-shaped connection in different cases

Cases	Influence coefficients range	Maximum variability
Case Y-1	0.547-0.574	4.94%
Case Y-2	0.555-0.571	2.88%
Case Y-3	0.555-0.559	0.72%
Case Y-4	0.555	0
Case Y-5	0.554-0.557	0.54%

As shown in Fig. 24 and Tab. 17, the Y-shaped connection contributes to reducing JD by approximately 50%, which can be explained by the same theory elaborated in Section 3.2. In addition, the influences of ground condition and pipe diameter on the influence

coefficients are more significant than those of the other three parameters. Herein, the safety of connection is guaranteed when the influence coefficient is 0.65 as suggested in Section 3.2.

4 Conclusions

This study analyzes the effect of pipe connection on the seismic JDs of buried segmented pipes by using the FEM. Five connections (cruciform and T-, K-, L-, and Y-shaped connections) and five group of parameters (ground condition, pipe diameter, branch angle, seismic incident angle, and input ground motion) are discussed in detail to provide comprehensive knowledge of the influence of connection on pipe JD. The influence coefficient, which measures the effect of connection on the seismic JD of a DCI pipe, is defined and calculated. On the basis of the analysis, the following conclusions can be drawn. (a) Comparing with the straight pipe, five pipe connections can reduce the seismic JD of a DCI pipe, and all the influence coefficients are nearly 0.5. (b) Different connections have different influence coefficients, and the relationships are T (K)>cruciform (Y)>L. For T (K) or cruciform (Y), the relationships maybe different in different scenarios. (c) Connection shape, ground condition, and pipe diameter influence the coefficients more significantly than branch angle, seismic incident angle, and input ground motion. (d) The safety of a pipe connection subjected to earthquakes can be guaranteed in engineering when the influence coefficient is 0.65.

Acknowledgement: The support from the National Key Research and Development Program of China (Grant No. 2016YFC0802400) is greatly appreciated.

Funding Statement: This research is supported by the Ministry of Science and Technology of China (Grant No. 2016YFC0802400). Wei Liu is the author who received the grant. The URLs to sponsors' website is http://www.most.gov.cn/.

Conflicts of Interest: The authors declare that they have no conflicts of interest to report regarding the present study.

References

Cao, Z.; Zhou, Y.; Xu, P.; Li, J. (2014): Mechanical response analysis and safety assessment of shallow-buried pipeline under the influence of mining. *Computer Modeling in Engineering & Sciences*, vol. 101, no. 5, pp. 351-364.

Datta, T. K. (1999): Seismic response of buried pipelines: a state-of-the-art review. *Nuclear Engineering and Design*, pp. 271-284.

Gan, S. W.; Hou, Z. L. (1988): Analysis of pipeline response to seismic wave propagation. *Earthquake Engineering & Engineering Vibration*, vol. 8, no. 2, pp. 79-85.

Han, Y.; Song, H. L.; Zhang, L.; Duan, J. F. (2010): Experimental research on ductile iron pipes with rubber gasketed joints. *Proceeding of Pipeline Division Specialty Conference*, pp. 1170-1176.

Hindy, A.; Novak, M. (1980): Pipeline response to random ground motion. *Journal of the Engineering Mechanics Division*, vol. 106, no. 2, pp. 339-360.

Japan Water Works Association (2009). *Guidelines and Commentary of Seismic Water Facilities and Constructions*. Japan Water Works Association, Tokyo, Japan.

Li, H. N.; Xiao, S. Y.; Huo, L. S. (2008): Damage investigation and analysis of engineering structures in the Wenchuan earthquake. *Journal of Building Structures*, vol. 29, no. 4, pp. 10-18.

Liu, W.; Li, J. (2008): Stochastic seismic response of pipelines with corrosion. *Journal of Earthquake Engineering*, vol. 12, no. 6, pp. 914-931.

Liu, W.; Miao, H. Q.; Wang, C.; Li, J. (2017): Experimental validation of a model for seismic simulation and interaction analysis of buried pipe networks. *Soil Dynamics and Earthquake Engineering*, vol. 100, pp. 113-130.

Liu, W.; Sun, Q. W.; Miao, H. Q.; Li, J. (2015): Nonlinear stochastic seismic analysis of buried pipeline systems. *Soil Dynamics and Earthquake Engineering*, vol. 74, pp. 69-78.

Liu, X. J.; Hou, Z. L. (1990): Seismic damage prediction and seismic measures of buried pipe network. *Proceeding of the 3rd National Symposium on Earthquake Engineering*, pp. 87-93.

Mandolini, A.; Minutolo, V.; Ruocco, E. (2001): Coupling of underground pipelines and slowly moving landslides by BEM analysis. *Computer Modeling in Engineering & Sciences*, vol. 2, pp. 39-47.

Miao, H. Q.; Liu, W.; Wang, C.; Li, J. (2016): Artificial earthquake test of gas supply networks. *Soil Dynamics and Earthquake Engineering*, vol. 90, pp. 510-520.

Ministry of Construction of the People's Republic of China (2003): *Code of Seismic Design of Outdoor Water Supply, Sewerage, Gas and Heating Engineering*. China Architecture and Building Press.

Nelson, I.; Weidlinger, P. (1979): Dynamic seismic analysis of long segmented lifelines. *Journal of Pressure Vessel Technology*, vol. 101, no. 1, pp. 10-20.

Newmark, N. M. (1967): Problems in wave propagation in soil and rock. *Proceeding of the International Symposium on Wave Propagation and Dynamic Properties of Earth Materials*, pp. 7-26.

Newmark, N. M.; Rosenblueth, E. (1971): *Fundamentals of Earthquake Engineering*. New Jersey.

O'Rourke, M. J.; Liu, X. (1999): *Response of Buried Pipelines Subject to Earthquake Effects*. New York: Multidisciplinary Center for Earthquake Engineering Research.

Pacific Earthquake Engineering Research Center (2017): http://peer.berkeley.edu/.

Sakai, H.; Pulido, N.; Hasegawa, K.; Kuwata, Y. (2017): A new approach for estimating seismic damage of buried water supply pipelines. *Earthquake Engineering & Structural Dynamics*, vol. 46, no. 9, pp. 1531-1548.

Shi, P. X. (2015): Seismic wave propagation effects on buried segmented pipelines. *Soil Dynamics and Earthquake Engineering*, vol. 72, pp. 89-98.

Shinozuka, M.; Koike, T. (1979): *Estimation of Structural Strains in Underground Lifeline Pipes*. NewYork: Department of Civil Engineering and Engineering Mechanics.

Singhai, A. C. (1984): Behavior of jointed ductile iron pipelines. *Journal of Transportation Engineering*, vol. 110, no. 2, pp. 235-250.

Singhal, A. C.; Zuroff, M. S. (1990): Analysis of underground and underwater space frame with stiff joints. *Journal of Computer and Structure*, vol. 35, no. 1, pp. 227-237.

Sun, Q. W.; Liu, W.; Li, J. (2012a): Analytical solution of soil spring constant for buried pipeline-soil lateral dynamic interaction. *Journal of Earthquake Engineering and Engineering Vibration*, vol. 32, no. 1, pp. 139-145.

Sun, Q. W.; Liu, W.; Li, J. (2012b): Soil spring costant of buried pipeline-soil longitudinal dynamic interaction. *Journal of Tongji University (Natural Science)*, vol. 40, no. 8, pp. 1123-1128.

Wang, C. (2015): *Field dynamic Test of Buried Pipeline Network with Explosive Simulating Earthquake* (*Ph.D. Thesis*). Tongji University, China.

Wang, C.; Liu, W.; Li, J. (2015): Artificial earthquake test of buried water distribution network. *Soil Dynamics and Earthquake Engineering*, vol. 79, pp. 171-185.

Wang, H. B.; Lin, G. (1988): Seismic response of the pipelines buried in three dimensional semi-infinite elastic medium. *China Civil Engineering Journal*, vol. 20, no. 3, pp. 80-91.

Wang, L. R. L. (1978): Vibration frequencies of buried pipelines. *Journal of the Technical Councils of ASCE*, vol. 104, no. 1, pp. 71-89.

Wang, L. R. L. (1979): *Some Aspects of Seismic Resistant Design of Buried Pipelines*. American Society of Mechanical Engineers.

Wang, L. R. L.; Cheng, K. M. (1979): Seismic response behavior of buried pipelines. *Journal of Pressure Vessel Technology. Transactions of the ASME*, vol. 101, no. 1, pp. 21-30.

Wang, L. R. L.; Lau, Y. C. (1989): Elasto-plastic seismic analyses of buried pipeline systems under ground shaking. *ASME Pressure Vessels Piping*, vol. 162, pp. 47-53.

Wang, L. R. L.; Pikul, R. R.; O'Rourke, M. J. (1982): Imposed ground strain and buried pipelines. *Journal of Pressure Vessel Technology. Transactions of the ASME*, vol. 108, no. 2, pp. 259-263.

Wang, L. R. L.; Wu, M. Z. (1991): Nonlinear dynamic seismic analysis of buried pipelines. *ASME Pressure Vessels and Piping Conference*, pp. 200.

Ye, F.; Guo, E. D.; Liu, J. L.; Liu, R. S. (2013): Seismic damage investigation and analysis of gas system in Lushan Ms 7.0 earthquake. *Journal of Natural Disasters*, vol. 22, no. 5, pp. 77-82.